

Separation of liquid mixtures in the freezing-out process—mathematical description and experimental verification

LEON GRADOŃ and DARIUSZ ORLICKI

Chemical Engineering Institute, Warsaw Technical University, Poland

(Received 16 April 1984)

Abstract—The analysis of the freezing-out process presented in Gradoń and Orlicki, *Int. J. Heat Mass Transfer* 27, 1141–1148 (1984) provided the basis for preparing the mathematical description of the separation of eutectic mixtures, taking into consideration the freezing effects taking place by supercooling. The results obtained from the numerical solution were compared with experimental data.

INTRODUCTION

OUR PREVIOUS paper [1] presented the mathematical description of the process of separating liquid mixtures, based on the separation of benzoic acid–naphthalene eutectic mixtures. The changes in physicochemical properties of the mixture occurring in the course of the process and caused by changes in local temperature and concentration in the phase boundary zone, were taken into account. The analytical forms of the functions describing changes in the values of coefficients present in balance transport equations were determined from the known correlations or by polynomial approximation of experimental results. This model allowed for sufficiently accurate analysis of the phenomena taking place during the freezing-out process and for determining the influence of particular controllable parameters on the efficiency of the separation process.

Due to the complex character of equations (i.e. nonlinear character of equation coefficients) the numerical analysis of the system of differential equations was also found to be complex. Besides the above model would not be easily adaptable for those separation processes where the influence of temperature and concentration on the process parameters (such as viscosity, diffusivity, heat conductivity) was unknown or only partly known.

Taking the above into account this paper presents a simplified version of the model and compares this to the general model when the latter applied to the same system undergoing the separation process.

In a later section of this paper the results computed using the mathematical model are compared with experimental results obtained while carrying out the investigated process in an apparatus designed specifically for this purpose.

MATHEMATICAL DESCRIPTION OF THE PROCESS

The liquid bi-componental alloy was placed in a sink provided with a mixer (Fig. 1). The temperature of a

liquid phase core was T_{∞} and the concentration of the freezing-out component was c_{∞} . A turning barrel was placed in the sink. The temperature of the barrel's wall was T_0 . Numerical calculations and experimental verification of the process were carried out for the eutectic mixture comprising naphthalene (N) and benzoic acid (K_b). The crystallization equilibrium curve for this system is presented on Fig. 2. Figure 3 illustrates the physical conditions of the model. By determining the quantitative dependencies of the process it was assumed that due to the barrel radius being much bigger than the thickness of the freezing-out layer the problem could be considered to be one-dimensional. Furthermore it was assumed that (a) the local thermodynamic equilibrium was reached on inter-phase boundary; (b) the centres of crystallization were uniformly arranged; and (c) temperature gradient and energy dissipation could be neglected. It was also assumed that no external forces were affecting the system.

In opposition to the general model the physicochemical parameters of liquid and solid mixtures were assumed to be constant within the investigated temperature range, along with the rate of flow in a liquid phase (plug flow).

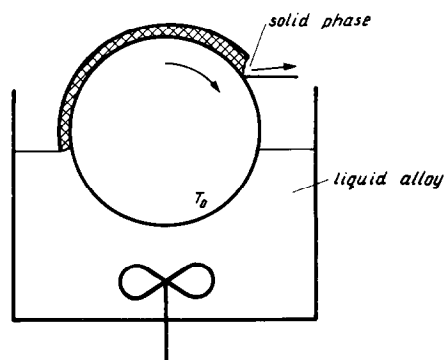


Fig. 1. The system for separation by freezing-out process.

NOMENCLATURE			
C	molar concentration [mol dm ⁻³]	Greek symbols	
c_p	specific heat [J kg ⁻¹ K ⁻¹]	α	occlusion coefficient
D	diffusion coefficient [m ² s ⁻¹]	δ	boundary-layer thickness [m]
H	heat of solidification [J kg ⁻¹]	λ	thermal conductivity [W m ⁻¹ K ⁻¹]
h	integration step	μ	viscosity [Pa s]
K	separation coefficient, C_s/C_l	ρ	mass density [kg m ⁻³].
T	temperature [K]	Subscripts	
t	time [s]	N	naphthalene
u	rate of solidification [m s ⁻¹]	K _b	benzoic acid
v	rate in the liquid alloy [m/s ⁻¹]	l	liquid
x	spatial coordinate	s	solid.
y	mole fraction.		

After analysing experimental results, the effects caused by the presence of a freezing alloy layer on the interphase boundary were taken into account in this model. The obtained results showed that these effects essentially influenced the freezing-out process because freezing did not lead to differentiation in the composition of the mixture.

Mass and energy balances were derived from the model of a boundary layer in inertial coordinates system related to the interphase boundary. Time unit Δt was the basis for all the balances given below. The chosen surface units in the balanced area were normal to the direction x along which the crystallization proceeded.

THE FREEZING-OUT PROCESS

Differential mass balance in the solid phase:

$$u(t) \frac{\partial C_{s,N}(x,t)}{\partial x} + \frac{\partial C_{s,N}(x,t)}{\partial t} = 0 \tag{1}$$

initial condition: $C_{s,N}(x,0) = 0$ (1)

boundary condition: $C_{s,N}(0,t) = C_{s,0}(t)$.

Differential energy balance in the solid phase:

$$\lambda_s \frac{\partial^2 T_s(x,t)}{\partial x^2} - u(t) \rho_s c_{ps} \frac{\partial T_s(x,t)}{\partial x} + \rho_s c_{ps} \frac{\partial T_s(x,t)}{\partial t} = 0 \tag{2}$$

initial condition: $T_s(0,0) = T_0$

boundary conditions: $T_s(0,t) = T_k(t)$ (2)

$$T_s[-u(t) \cdot t, t] = T_0.$$

Differential mass balance in the liquid alloy:

$$-D_{N,K_b} \frac{\partial}{\partial x} \left[C_l(x,t) \frac{\partial}{\partial x} y_N(x,t) \right] - u(t) \frac{\rho_s}{\rho_l} \times \frac{\partial C_{l,N}(x,t)}{\partial x} + \frac{\partial C_{l,N}(x,t)}{\partial t} = 0 \tag{3}$$

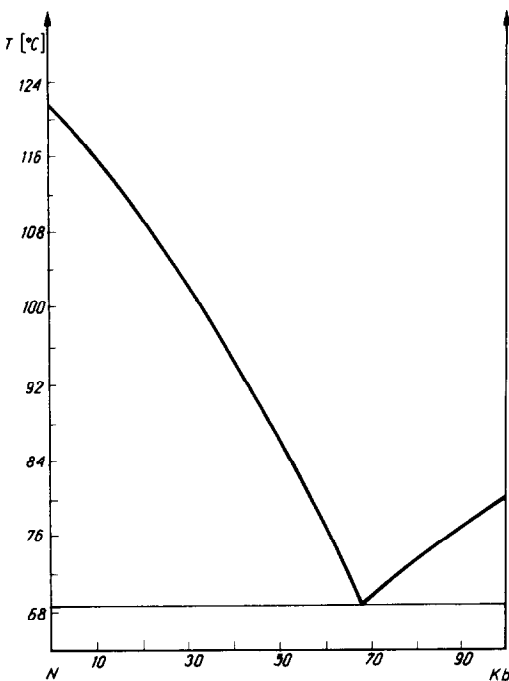


FIG. 2. Distribution of temperature and concentration in boundary layers.

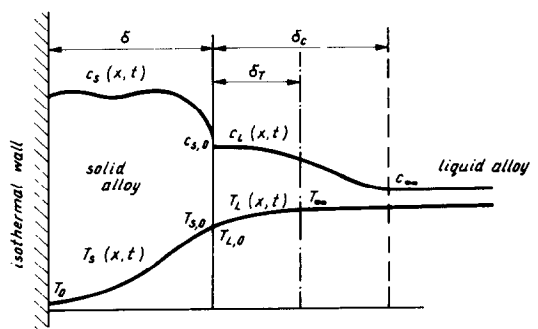


FIG. 3. Crystallization equilibrium curve of naphthalene-benzoic acid mixture.

$$\begin{aligned} \text{initial condition: } & C_{1,N}(x, 0) = C_\infty \\ \text{boundary conditions: } & C_{1,N}(0, t) = C_{1,0}(t) \\ & C_{1,N}(\delta_c, t) = C_\infty. \end{aligned} \quad (3')$$

Differential energy balance in the liquid alloy:

$$\begin{aligned} \lambda_1 \frac{\partial^2 T_1(x, t)}{\partial x^2} - u(t) \rho_s c_{pl} \frac{\partial T_1(x, t)}{\partial x} + (D_{K_b, N} M_{K_b} c_{pl, K_b} \\ - D_{N, K_b} M_N c_{pl, N}) \frac{\partial}{\partial x} \left[C_1(x, t) T_1(x, t) \frac{\partial}{\partial x} y_N(x, t) \right] \\ + \rho_1 c_{pl} \frac{\partial T_1(x, t)}{\partial t} = 0 \end{aligned} \quad (4)$$

$$\begin{aligned} \text{initial condition: } & T_1(x, 0) = T_\infty \\ \text{boundary conditions: } & T_1(0, t) = T_k(t) \\ & T_1(\delta_t, t) = T_\infty. \end{aligned} \quad (4')$$

Differential mass balance on the interphase boundary:

$$\begin{aligned} u(t) C_{s,0}(t) + u(t) \frac{\rho_s}{\rho_1} C_{1,0}(t) \\ + D_{N, K_b} C_{1,0}(t) \frac{\partial y_N(x, t)}{\partial x} \Big|_{x=0} = 0 \end{aligned} \quad (5)$$

$$C_{1,0}(t) = f_1[T_k(t)] \quad (5')$$

$$C_{s,0}(t) = [1 - \alpha(t)] \cdot f_s[T_k(t)] + \alpha(t) \cdot f_l[T_k(t)]. \quad (5'')$$

Differential energy balance on the interphase boundary:

$$\begin{aligned} -\lambda_s \frac{\partial T_s(x, t)}{\partial x} \Big|_{x=0} - u(t) \cdot \rho_s c_{ps} [T_k(t) - T_{0d}] \\ + \lambda_1 \frac{\partial T_1(x, t)}{\partial x} \Big|_{x=0} + u(t) \rho_s c_{pl} [T_k(t) - T_{0d}] \\ + (D_{N, K_b} M_N c_{pl, N} - D_{K_b, N} M_{K_b} c_{pl, K_b}) C_1(0, t) \\ \times [T_k(t) - T_{0d}] \frac{\partial y_N(x, t)}{\partial x} \Big|_{x=0} + u(t) \rho_s M(t) = 0. \end{aligned} \quad (6)$$

THE FREEZING PROCESS

Mass balance on the interphase boundary:

$$\begin{aligned} C_{1,0}(t) = f_1[T_k(t)] \equiv C_\infty \quad (7) \\ C_{s,0}(t) = f_s[T_k(t)]. \quad (8) \end{aligned}$$

The difference in concentration values [equation (8)] is due to the changes in volume caused by phase transition process.

Differential energy balance on the phase boundary:

$$T_k(t) = T_E \quad (9)$$

$$\begin{aligned} -\lambda_s \frac{\partial T_s(x, t)}{\partial x} \Big|_{x=0} - u(t) \rho_s c_{ps} [T_k(t) - T_{0d}] \\ + \lambda_1 \frac{\partial T_1(x, t)}{\partial x} \Big|_{x=0} + u(t) \rho_1 c_{pl} [T_k(t) - T_{0d}] \\ + u(t) \rho_1 M(t) = 0. \end{aligned} \quad (10)$$

The numerical values of the coefficients present in equations (1)–(10) were taken from ref. [2]. Their values used in the computations were chosen so as to represent the mean values of the applied range of thermodynamic parameters of the process.

The occlusion coefficient α was defined as the ratio of the volume of the liquid phase enclosed in the solid phase to the total volume of crystalline phase, according to the equation (11):

$$\alpha(t) = A + B \exp \left[\frac{C}{u(t)} \right]. \quad (11)$$

This equation was derived from theoretical model of occlusion [4] based on the crystallization mechanism involving the formation of dendrite structures and interference of dendrites from adjoining crystals. The conditions leading to the loss of the form stability of crystals were given in ref. [5].

Numerical computations of the system of equations were carried out by the Crank–Nicholson method. The conditions and differential scheme were the same as in ref. [1].

The following values of the parameters (external) were used by computations:

$$\begin{aligned} T_\infty = 358.16 \text{ K} \quad C_\infty = 7019.8 \text{ mol m}^{-3} \\ T_{01} = 341.36 \text{ K} \quad T_{02} = 338.16 \text{ K} \\ \delta_c = 2.9 \times 10^{-4} \text{ m} \quad \delta_t = 5 \times 10^{-5} \text{ m} \\ A = 0, \quad B = 0.1, \quad C = -0.472 \times 10^5. \end{aligned}$$

As was shown in our previous paper the separation efficiency determined by the separation coefficient K (defined as the ratio of the component concentration in the liquid phase to its concentration in the solid phase under equilibrium conditions) could be increased by introducing a device controlling the temperature of the barrel wall. Both descriptions of the two-zone freezing-out process wherein the temperature of the barrel wall are T_{01} and T_{02} , are compared below. The results of the computations are presented on Figs. 4–7.

The curves illustrate the changes in separation coefficient K , temperature of solidification area T , rate of solidification $u(t)$ and thickness of the solid-phase layer with the real time of the process. They present the changes in the key parameters of the freezing-out process. It may be seen that simplifying the model only slightly influences the final results. In every case the relative error determined with regard to the accurate model does not exceed 10%. In the next part the experimental results are compared with the results obtained when using the simplified model of the freezing-out process.

THE COMPARISON OF EXPERIMENTAL RESULTS WITH MATHEMATICAL DESCRIPTION

Figure 8 shows the scheme of apparatus wherein the experimental researches were carried out. The main

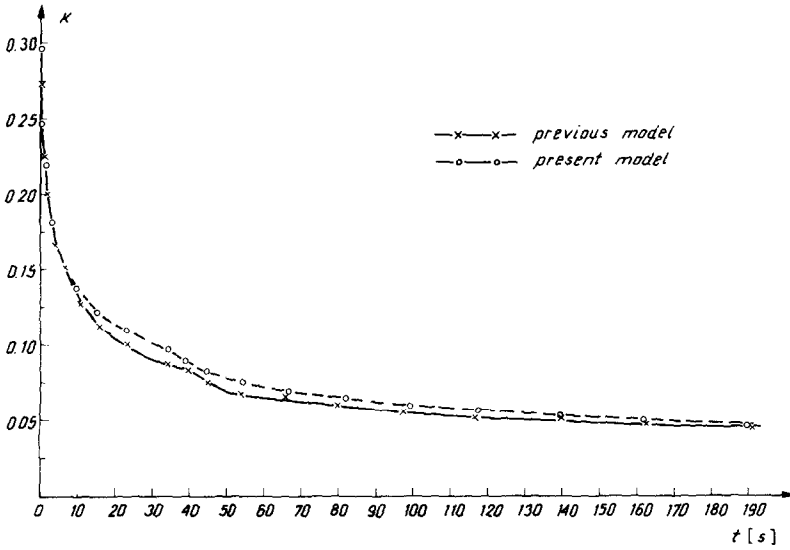


FIG. 4. Dependence of separation coefficient on time.

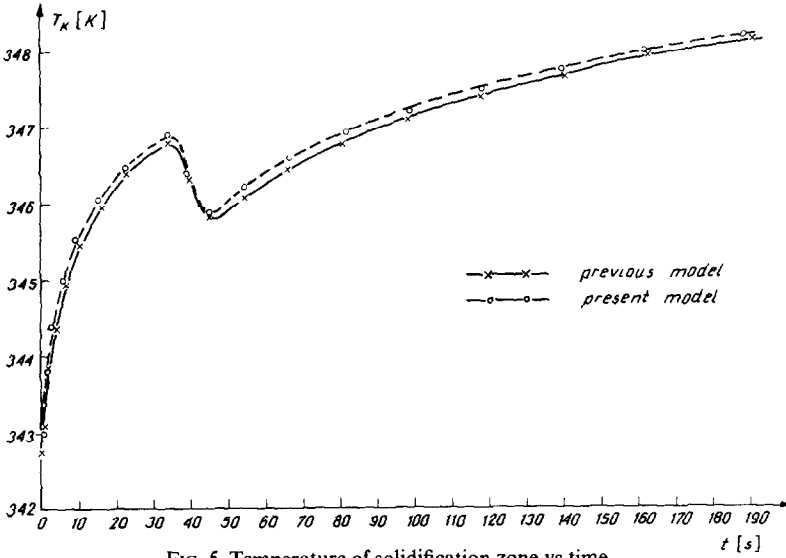


FIG. 5. Temperature of solidification zone vs time.

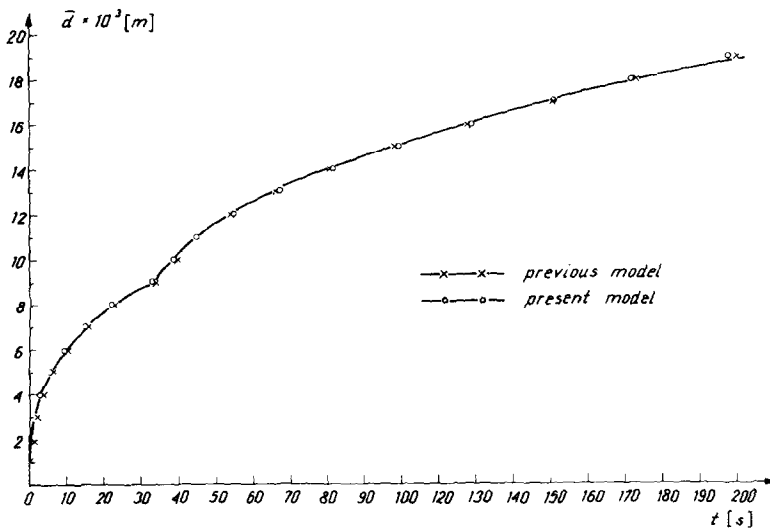


FIG. 6. Rate of solidification vs time.

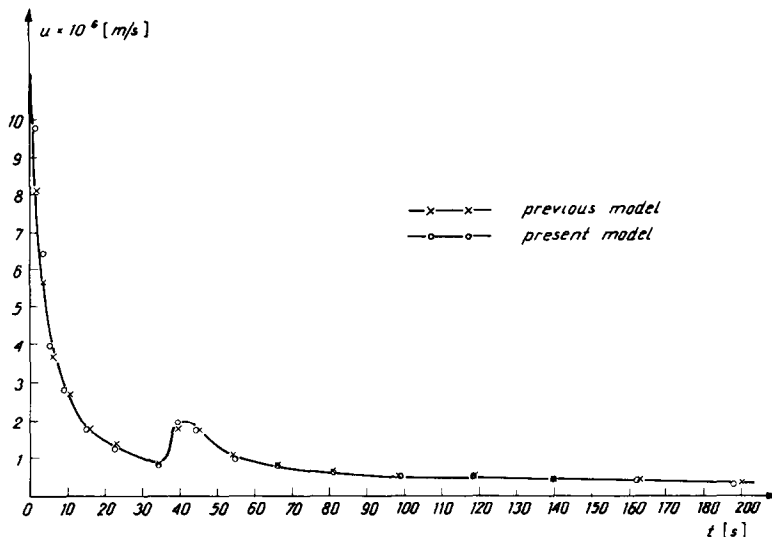


FIG. 7. Thickness of solid-phase layer vs time.

element is the barrel 1 placed in the sink 2 of the thermostat. The barrel's surface is cooled by the cooling medium flowing over its wall. Inside the barrel are the elements, profiled to direct the flow of the cooling medium. The front walls of the barrel are heat insulated in order to prevent crystallization thereon. The cooling medium flows into and from the barrel in concentric pipes placed along its axis.

The barrel is rotated at the appropriate speed using a suitably geared electrical drive 5. The system is also equipped with devices for controlling temperature of an alloy in the sink, of the barrel wall and the thickness of the frozen-out layer.

The naphthalene-benzoic acid alloy of a desired composition is placed in the sink 2. After melting, its temperature settles at T_∞ and the temperature of the barrel wall at T_0 . The barrel drive system is switched on to give the appropriate speed of rotation. When the layer of solid phase on the barrel wall reaches its desired thickness, a section of it is removed for analysis. At the

same time a sample of liquid alloy is also removed for analysis.

The samples are analysed by titration of their benzene solutions with 0.1 N aqueous NaOH solution in the presence of phenolphthalein. Figure 9 presents the results of computing the separation coefficient K for the mixtures of naphthalene and benzoic acid separated by the freezing-out process carried out in the one-step barrel freezer, based on the above mathematical model of this process. The parameters of the process are given below:

$$T_0 = 335.46 \text{ K} \quad T_\infty = 358.16 \text{ K}$$

$$C_\infty = 7019.8 \text{ mol dm}^{-3} \quad \delta_1 = 1.6 \times 10^{-4} \text{ m.}$$

The figure presents the curves obtained using different values of occlusion coefficient α . Its theoretical value is computed using the theory assuming the stability of form of the growing dendrites. The curves 1-4 relate to the cases wherein the changes in α values lie within the range applied during the process.

The characteristic increase in the value of separation coefficient (curves 2, 3 and 4) takes place by passing from the conditions under which the freezing of the solution takes place to the conditions under which the freezing-out occurs.

When the first-stage periods of time are short (freezing effect) due to the small thickness of the freezing layer, the extreme value of K is observed when the time required for conducting the process is short.

After this stage the coefficient decreases in an asymptotic way to its primary settled value. The value of K increases rapidly only by the particular driving force of the process, implying the rate $u(t)$, α coefficient and the shape of its curve (more or less broadened) changes according to the changes in the process conditions.

The values of A , B and C , present in equation (11),

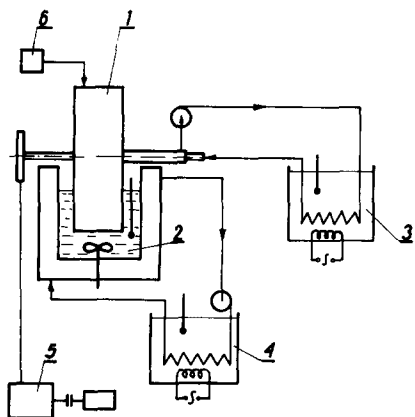


FIG. 8. Scheme of control device.

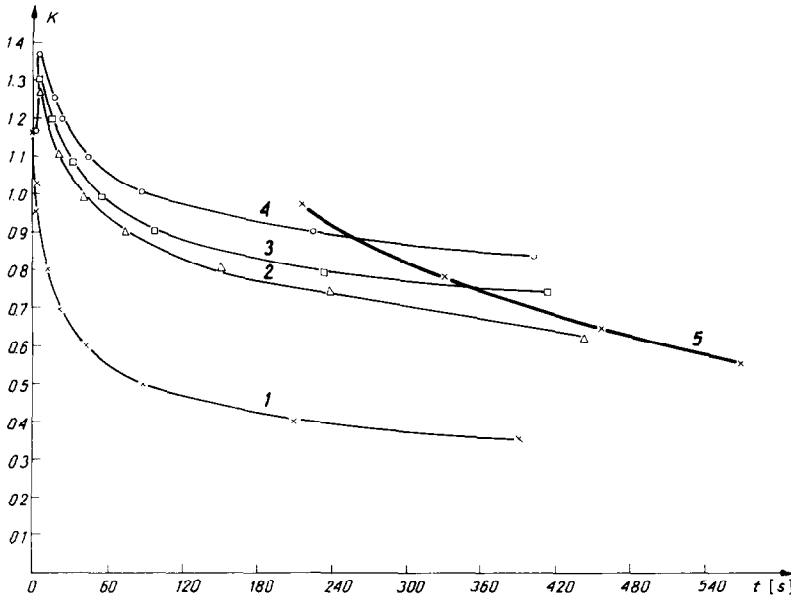


FIG. 9. Comparison of computed and experimentally determined separation coefficient vs time.

used for computing α are given below:

	A	B	C
1	0	0.1	-0.472×10^{-5}
2	3×10^{-2}	0.5	-0.472×10^{-5}
3	3×10^{-2}	0.55	-0.472×10^{-5}
4	3×10^{-2}	0.6	-0.472×10^{-5}

Curve 5 on Fig. 9 presents the experimental results obtained under conditions applied by numeric computations. The technological conditions of the process require the chosen freezing-out time periods to lie within their upper range. Under these conditions the obtained values of the thickness of solid-phase layers ensure higher accuracy of measurements. The comparison of experimental results with the model indicates that the model approximates the real progress of the process with sufficient accuracy. Determination of the accurate value of the occlusion coefficient, which greatly influences the efficiency of separation, requires further analysis.

Up to now solutions of Stefan's problem explain the differences between the experimental results and the theoretical description by the influence of α and its values are chosen so as to achieve compatibility. In order to avoid this the values of α introduced into our

computations were found out from theoretical methods.

SUMMARY

The presented results allow for the assumption that the proposed simplified model of separating liquid mixtures by freezing-out process sufficiently approximates the real progress of this process. As in order to compute the process according to this model it is necessary to consider only external controllable process parameters and the values of transport parameters that can be found in the tables, it may be found useful by pre-planning such separation systems.

REFERENCES

1. L. Gradoń and D. Orlicki, Liquid mixtures separation in a freezing-out process, *Int. J. Heat Mass Transfer* **27**, 1141–1148 (1984).
2. R. H. Perry and C. Chilton, *Chemical Engineers Handbook* (5th edn). McGraw-Hill, New York (1974).
3. L. Gradoń, Mechanism of dendrite formation, Chemical Engineering Conference, Lodz (1980).
4. E. Plóciennik, Masters thesis, Warsaw Technical University (1980).
5. J. S. Langer, Dendritic solidification of dilute solutions, *PhysChem. Hydrodynam.* **1**, 41–49 (1980).

SEPARATION DES MELANGES LIQUIDES PAR CONGELATION— DESCRIPTION MATHÉMATIQUE ET VÉRIFICATION EXPÉRIMENTALE

Résumé—Nous présentons ici la description mathématique de la séparation du mélange eutectique, en prenant en considération l'effet de congélation qui a lieu à des plus fortes surfusion. Nous nous basons sur les résultats de l'analyse de la frigidation compris dans le travail [1]. Les résultats de la solution numérique du problème ont été comparés avec l'expérience.

TRENNUNG FLÜSSIGER GEMISCHE DURCH AUSFRIEREN—MATHEMATISCHE
BESCHREIBUNG UND EXPERIMENTELLE BESTÄTIGUNG

Zusammenfassung—Es wird das mathematische Modell der Trennung eines eutektischen Gemisches vorgestellt, wobei Erstarrungseffekte bei Unterkühlung berücksichtigt sind. In dem Modell werden die in der Arbeit [1] beschriebenen Ergebnisse der theoretischen Untersuchungen des Ausfrierverfahrens angewandt. Die Ergebnisse der numerischen Lösung des Problems wurden mit experimentellen Daten verglichen.

РАЗДЕЛЕНИЕ СМЕСЕЙ ЖИДКОСТЕЙ В ПРОЦЕССЕ ВЫМОРАЖИВАНИЯ.
МАТЕМАТИЧЕСКОЕ ОПИСАНИЕ И ЭКСПЕРИМЕНТАЛЬНАЯ ПРОВЕРКА

Аннотация—Анализ процесса вымораживания, представленный в [1], создает основу для математического описания разделения эвтектических смесей с учетом эффектов замерзания, имеющих место при переохлаждении. Данные, полученные в результате численного решения, сравниваются с экспериментальными.